Flight Testing a Highly Flexible Aircraft: Case Study on the MIT Light Eagle

S. H. Zerweckh* and A. H. von Flotow†
Massachusetts Institute of Technology, Cambridge, Massachusetts 02139
and
J. E. Murray‡
NASA Ames Research Center, Edwards, California 93523-5000

This paper describes the techniques developed for a flight test program of a human powered aircraft, the application of these techniques, and the results of the flight testing. A system of sensors, signal conditioning, and data recording equipment was developed and installed on the aircraft. Flight test maneuvers that do not exceed the aircraft's limited capability were developed and refined in an iterative sequence of test flights. The test procedures were adjusted to yield maximum data quality from the point of view of estimating lateral and longitudinal stability derivatives. Structural flexibility and unsteady aerodynamics are modeled in an ad hoc manner capturing the effects observed during the test flights. A model with flexibility extended equations of motion is presented. Results of maneuvers that were flown are compared with the predictions of that model and analyzed. Finally the results of the flight test program are examined critically, especially with respect to future applications, and suggestions are made in order to improve maneuvers for parameter estimation of very flexible aircraft.

I. Introduction

ON January 22, 1987, the MIT (Massachusetts Institute of Technology) Light Eagle extended the world distance record for human-powered aircraft to almost 60 km serving as a testbed for the follow-on airplane Daedalus, which extended the distance record even further to 130 km during spring 1988. For flight tests conducted in the winter of 1987–1988, the Light Eagle was equipped with a variety of sensors such as strain gauges, accelerometers, rate gyros, control surface potentiometers, and an onboard data acquisition system. The test phase covered by this paper had three major objectives. The first objective was pilot training. The pilots should become familiar with the aircraft and experience its characteristics during flight. The second objective was to verify that the data acquisition system and the sensors were working properly. Both systems were unique in terms of weight and data density. The third objective was to collect data on the aeroelastic behavior, aerodynamic performance, and handling qualities of the aircraft.

Although human-powered aircraft are interesting vehicles, it seems unlikely that they will become practical flying machines with widespread application. They are, however, prototypical of a class of aircraft that may soon be in widespread use[1]: high altitude, high endurance aircraft. These aircraft will need to be very light and aerodynamically efficient in order to stay aloft for long periods with onboard fuel or with solar or microwave power. They will have a high aspect ratio and fly subsonically at Reynolds numbers comparable to those of human powered aircraft. One might thus view the research reported here as being prototypical of that required for development of such high altitude, high endurance aircraft.

II. Unique Features of the Light Eagle

The Light Eagle (see Fig. 1) is a unique aircraft. Its design flight speed is approximately 7.8 m/s (15 mph, $Re = 500{,}000 - 200{,}000$), at a lift to drag ratio of 36. The aspect ratio of 39.4 is one of the highest ever flown and is achieved in spite of the very low empty weight of 42 kg (88 lb), approximately one-third of the maximum gross weight. The structure, based on graphite-epoxy spars (which are the load-carrying structure), foam ribs, foam leading-edge inserts, and a mylar skin (which gives the aerodynamic shape), is driven as much by stiffness as by strength requirements. The wing is braced by a single lift wire, a compromise between structural and aerodynamic considerations. The power required to maintain level flight is approximately 230 W (0.31 hp) at a total weight of 110 kg (242 lb) (see Table 1).

Pilot-Induced Oscillations

The pilot is the aircraft's powerplant as well as the control unit. In his role as a powerplant, the pilot must pedal, reciprocating his legs (perhaps 21 kg or 20% of the gross aircraft weight) through a distance of some 40 cm. The pedaling frequency is about 2 Hz for some pilots coinciding with a natural structural frequency (coupled chordwise bending/torsion of the wing and tail-boom bending in the up-down direction). The pilot thus introduces a large periodic signal into all instrumentation channels, precisely in the frequency range of interest. For this reason, much of the flight testing was done during unpowered gliding flight with the aircraft being towed to a certain altitude and then released.

Apparent Mass Effects

The Light Eagle flies with a wing loading of 37 N/m^2 (see Table 2). The weight of the volume of air enclosed in a cylinder

Presented as Paper 88-4375 at the AIAA Atmospheric Flight Mechanics Conference, Minneapolis, MN, Aug. 15-17, 1988; received Nov. 14, 1988; revision received Aug. 22, 1989.

*Research Assistant, Department of Aeronautics and Astronautics. Student Member AIAA.
†Associate Professor, Department of Aeronautics and Astronautics. Member AIAA.
‡Research Engineer, Dryden Flight Research Facility.

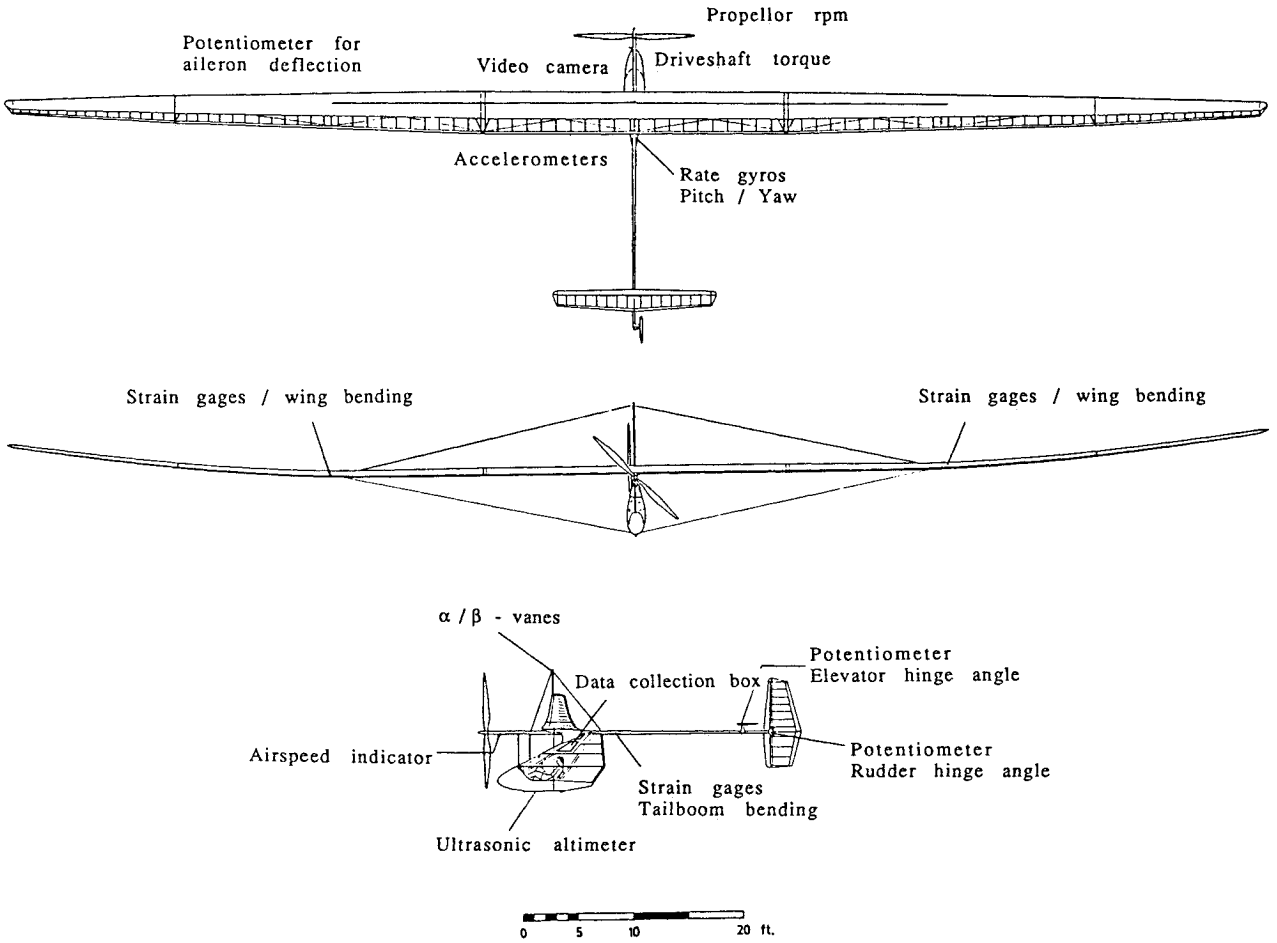

Fig. 1 Sensor positions and research instrumentation.

with its diameter equal to the chord and its length equal to the span is approximately twice the wing weight. Apparent mass effects are thus large, must be consistently included in dynamic models, and have large influence upon control procedures—particularly lateral control (see Table 3). The mass of air inside the wing is in itself 25% of the wing mass and contributes strongly to the yawing and rolling moments of inertia of the aircraft.

Table 1 Light Eagle, Gossamer Albatross II, and Stork B

	Light Eagle	Gossamer Albatross II	Stork B
Wing area, m^2	31	44	21.7
Drag area, m^2	0.8	2.5	0.7
Wing span, m	34.7	29	21
Aspect ratio	39.4	18.9	20.3
Empty weight, kg	42	32	35.9
Design power, W			
Clean	230	246	275
Dirty	275	./.	./.
Design airspeed, m/s	7.8	5.0	8.6

Table 2 Wing loading of different aircraft

High performance sail planes, N/m^2	372-395
Trainer sail planes, N/m^2	214
Hang gliders, N/m^2	38-67
Light Eagle, N/m^2	37

Aircraft Flexibility

Unloaded, the aircraft's wing spar is straight. Equilibrium tip deflections during level flight exceed 1.4 m (4.6 ft) almost entirely due to wing bending outboard of the lift wire. This curved equilibrium shape must be taken as the reference configuration for linearized dynamic analysis. Coupling between chordwise bending and torsion is created by this curvature leading to the potential of an unusual flutter mode involving chordwise motion.[2,3] The flexibility of the tail boom is very important for the coupling of lateral rigid-body modes and flexible modes and induces a considerable time delay between rudder and elevator control input and the airplane response. Above a certain frequency, empennage control inputs have little effect on the overall motion of the aircraft and solely excite structural modes of the tailboom.

The aircraft structural natural frequencies are comparable with (and even slower than) the rigid-body estimates of the short period and the Dutch roll modes. One must thus expect that flexibility will play a large part in the aircraft dynamic response and that rigid-body motion will contribute to aeroelastic behavior.[4] Table 4 is a summary of estimates of aircraft natural frequencies, generated by a finite-element analysis of the aircraft structure.

Unsteady Aerodynamics

The chord-based reduced frequency corresponding to a frequency of 1 Hz, a flight speed of 8 m/s, and a chord of 0.8 m is $k = \omega c/u = 0.63$. This implies that unsteady aerodynamic effects will play a major role in the dynamic response of the aircraft for all motions above, say, 0.1 Hz. This frequency is well within the pilot's bandwidth and within the spectrum of the control inputs used during flight testing.

Table 3 Light Eagle mass and inertias

Fuselage with tailboom, kg (lb)	14.3	(31.5)
Wing, kg (lb)	22.3	(49.1)
Tail surfaces, kg (lb)	1.6	(3.7)
Complete instrumentation, kg (lb)	2.5	(5.5)
Data acquisition system alone, kg (lb)	1.0	(2.2)
Air mass/length, enclosed in wing, kg/m (lb/ft)	0.16	(0.1)
Wing mass/length, kg/m (lb/ft)	0.62	(0.43)

Without apparent mass		With apparent mass	
I_x, kgm^2	2002	I_x, kgm^2	392
I_y, kgm^2	205	I_y, kgm^2	340
I_z, kgm^2	2086	I_z, kgm^2	2910

Table 4 Aircraft structural natural frequencies

Mode number	Frequency, Hz	Description
1	0.0	Rigid-body X translation
2	0.0	Rigid-body Y translation
3	0.0	Rigid-body Z translation
4	0.0	Rigid-body rotation about X axis
5	0.0	Rigid-body rotation about Y axis
6	0.0	Rigid-body rotation about Z axis
7	0.559	1st symmetric wing bending
8	0.677	Tail-boom rotation
9	0.879	1st asymmetric wing bending
10	1.134	1st symmetric wing bending (fore aft)
11	1.183	1st tail-boom bending (X-Y plane)
12	2.267	1st tail-boom bending (X-Z plane)
13	2.336	2nd symmetric wing bending
14	2.603	2nd asymmetric wing bending
15	2.919	1st wing asymmetric torsion
16	4.147	3rd wing symmetric bending

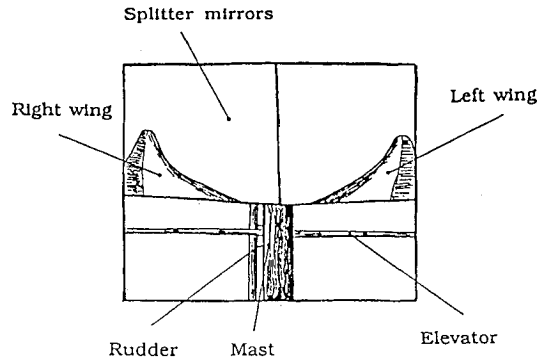

Fig. 2 Video images.

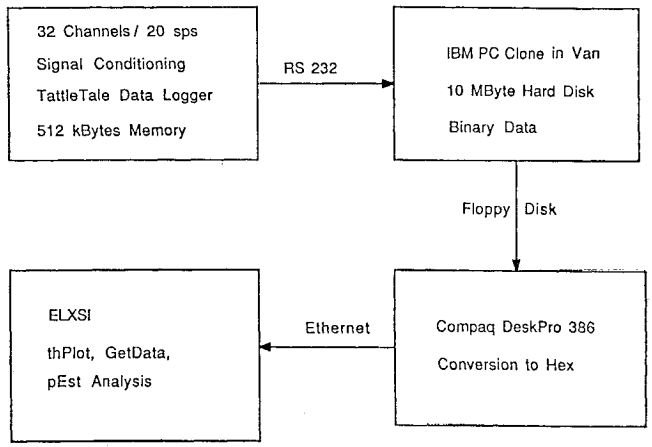

Fig. 3 Data acquisition system.

III. Flight Testing

The research flights started in late December 1987 with a shakedown of the Light Eagle instrumentation and all of the data transfer links. An accident on Rogers Dry Lakebed, Edwards Air Force Base, California, on February 7, 1988, with the Dae-dalus 87 aircraft influenced the Light Eagle flight test program to some degree. More emphasis was placed on lateral stability and control characteristics than would have otherwise been done, and flight testing was extended four weeks.

The flight test program ended in mid-March 1988 after the major goals of the program had been achieved.

Flight Test Instrumentation

Figure 1 shows the sensors and instrumentation that were installed on board the aircraft. All channels are analog filtered with a single pole filter (break frequency 5 Hz) and are sampled at 20 Hz. Data are stored on board in a solid-state memory[5] and downloaded into a portable PC installed in the back of the chase vehicle. Data analysis was done on one of NASA's mainframe computers.

A video camera, mounted above the main fuselage tube in front of the wing and looking aft, imaged empennage and both wings, via mirrors, simultaneously (see Fig. 2). The video images were primarily used to detect the more distinct natural modes of the aircraft structure visually in order to get a better understanding about the importance of these modes. The video images were also used to compare the results of the finite-element analysis with the observed modes.

Strain gauges on the main wing spar and the tail boom provided information about the deflections of major structural parts. Rate gyros were attached to the fuselage tube that supported the back of the pilot's seat. The attachment was designed to allow the gyros to rotate 90 deg in order to use them in different axes and to be able to cross check the gyro output signals. The pitch gyro, for instance, could be rotated in its plane of sensitivity and thus also be used as roll gyro. The mount for the second gyro was designed in the same way so that yaw and pitch motion could be detected with this arrangement. This enabled changing the gyros' axes of sensitivity such that the two main axes of motion were monitored according to whether a lateral or longitudinal maneuver was performed. The flight test instrumentation, weighing about 2.5 kg (5.5 lb) with power supply, also included two accelerometers, mounted next to the rate gyros, which could be turned in order to be aligned with the axes of motion. The accelerometer output signals could also be cross checked when they were both aligned in the same axis. Although the accelerometers were not mounted at the mass center, they provided good results, even without compensation, during the parameter estimation process. The parameter estimates were not noticeably affected by a difference between the mass center location and the accelerometer position of less than 0.5 m.

A unique feature of the data acquisition system is the light weight (approximately 1 kg) and the high data storage capacity (512 kbyte) on board the aircraft. The data collection and storage computer is approximately the size of a cigarette package and communicates with a PC through an RS 232 connection.

Data Reduction

One of the important features of the data reduction was speed. The tattletale computer, which stored binary data in a 512 kbyte RAM chip, was able to download the data at 9600 baud into the portable PC. The download time was approximately equal to the time of the test flights. With the PC, the data were stored on floppy disks. At noon time, the data from the morning's flights were converted into hexadecimal format and loaded onto a mainframe computer at NASA. This proce-

Table 5 Flight test matrix

Control inputs	Flight conditions: Unpowered towed flights	Powered flights 15 mph	Powered flights 18 mph	Long liftwire	Short liftwire	Comments
Elevator doublet, Hz	2	2	2	—	*	Good data
Rudder doublet, Hz	2	2	2	*	—	Poor roll axis gyro data
Aileron doublet, Hz	0.5	0.5	0.5	—	*	Ailerons nonlinear
Elevator frequency sweep, Hz	0–3	0–3	0–3	—	*	Good data
Rudder frequency sweep, Hz	0–3	0–3	0–3	*	*	Good data
Aileron frequency sweep, Hz	0–1	0–1	0–1	—	*	Not used because of nonlinearities and "sticky" aileron hinges
Dutch roll rudder/aileron doublet	1	1	1	—	*	

dure enabled reduction of the data sets from the morning flights on the same day (see Fig. 3). Time history plots of all the test flights together with preliminary parameter identification results were ready for a pilot debriefing in the evening. Another advantage was the ability to respond very quickly to new ideas and inputs from the engineers as well as from the pilots. Thus every possible flight day was used for test flights; approximately 150 flights were conducted in three months. During this time, 30 flights produced a data base for analysis. Among these 30 "data flights," 9 were used to estimate stability derivatives. The rest of the data base proved to be of insufficient quality for stability parameter estimation, but was used for qualitative examination of the aircraft's behavior. It has to be pointed out that the 9 flights contain approximately 50 maneuvers (e.g., rudder doublets, elevator doublets, frequency sweeps).

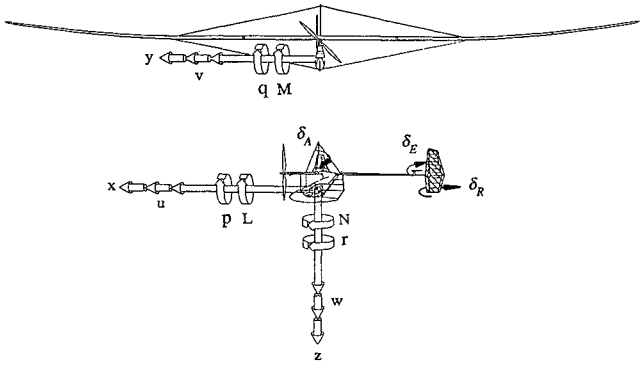

Fig. 4 Vehicle-axis system and notation.

Flight Test Maneuvers

The flight test maneuvers were severely constrained by safety and operational considerations. The aircraft is marginally powered and has a fairly small structural safety margin. The Light Eagle typically flies at 3–4 m (10–16 ft) altitude and is designed to operate in a narrow speed range of 6.6–9.1 m/s (13–18 mph). Table 5 is a presentation of the flight test matrix with the first column (unpowered towed flights) the one with the highest priority. Figure 4 gives an illustration of the aircraft-axis system and the notation used in the analysis.

All test flights were made in the early morning in an attempt to avoid turbulence and thermal activity. Thus, time available for flight testing was limited to about 3 h every morning. The effects of solar heating on the lake bed became significant after about 10:00 a.m., contaminating mostly the angle-of-attack data. Most of the data sets used for parameter identification were taken on extremely calm and overcast days. A schedule for a typical flight day was

1) Preflight pilot briefing the evening before the flight. Presentation of the flight test data from the day before and discussion with the pilots about how to improve the maneuvers.

2) Towed flight with climb to 30–40 ft altitude, release the tow line, and establish steady-state flight conditions.

3) Start tattletale computer and activate sensors.

4) Execute flight test maneuver and repeat the maneuver after having again established steady-state flight conditions.

5) Land the aircraft, stop the tattletale computer, and download flight test data onto the floppy disk of the PC in the chase van (download time was equal to the time during which data were taken: typically 3–5 min).

6) Turn around and repeat the test cycle.

The maneuvers performed by the pilots (Kanellos Kanellopoulos, Erik Schmidt, Frank Scioscia, Glenn Tremml, and Greg Zack) were as follows.

Steady Turns

The main purpose of this maneuver was to collect data on the sideslip angle during a steady-state turn. Preliminary test

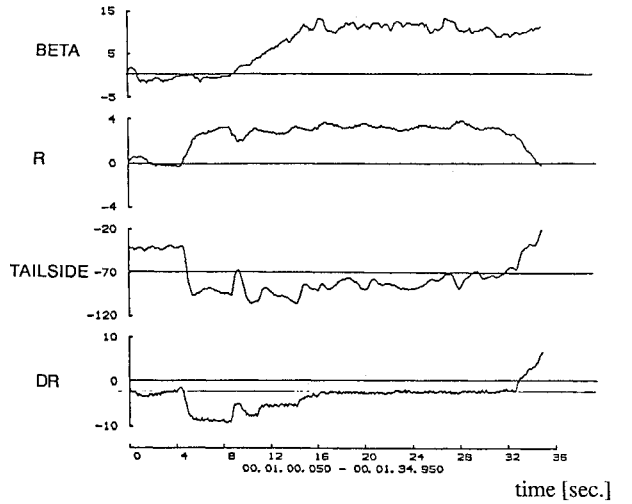

Fig. 5 Steady-state turn, rudder only.

flights indicated that the steady-state sideslip angle was much higher than predicted and that this contributed to the Daedalus 87 accident. Another data set was recorded: flying with rudder and ailerons in order to compare both maneuvers and assess the value of ailerons for lateral control (see Fig. 5). This maneuver demonstrated the ability to control the aircraft during a nominal turn with rudder only. Starting at $t_{start} = 4$ s, the aircraft establishes an almost constant yaw rate of 3 deg/s. Roll angle into the turn and sideslip angle builds up steadily until at $t = 16$ s, a steady turn is established with a constant rudder setting of approximately 3 deg, into the turn. The high angle of sideslip throughout the maneuver is remarkable. It builds up gradually and remains constant during the turn at approximately 12 deg. The aircraft has rolled too far and performs a "slipping" turn.

Control Surface Pulses and Doublets

These maneuvers were conducted in all three axes and were especially helpful in judging the effectiveness of the rudder vs ailerons. The comparison between a rudder and an aileron doublet was of particular interest because the Daedalus aircraft did not have ailerons and therefore needed to be controllable in the lateral axis with rudder only via roll/yaw coupling (see Fig. 6). The time-history plot shows two control surface doublets. The aileron doublet starts at $t_{start} = 5$ s and ends at $t_{end} = 13$ s. It is followed by a rudder doublet with a duration of 5 s. The other two channels show the fuselage response in yaw rate and roll rate. These plots demonstrate the significant adverse yaw effect of the ailerons showing that the yaw rate signal is about 4 deg/s opposite to the desired turn, and the roll rate signal is only -1 deg/s. Rudder deflection, on the other hand, rolls and yaws the aircraft toward a coordinated turn.

These maneuvers were used for parameter identification using a rigid aircraft model with quasisteady aerodynamics. During the test flights, it was obvious that the high flexibility of the aircraft's main structure, namely tail boom and wing spar, invalidate the rigid assumption. The equations of motion were extended by introduction of a first-order filter between control surface deflection and application of control torque. The doublet maneuvers accentuate this time lag and were used to estimate the additional parameters of the filter.

Frequency Sweeps

Control surface frequency sweeps were conducted in all three axes. Frequency sweeps with rudder and ailerons helped to evaluate the interaction between rigid-body modes and aircraft flexibility. Previous test flights had shown that the aircraft responds fairly quickly in the pitch axis, whereas in roll and yaw (lateral-directional) the response is very slow and is affected by structural flexibility of the tail boom and the wing. Figure 7 shows an elevator frequency sweep starting with steady-state flight conditions at $t = 12$ s with a frequency of approximately 0.3 Hz gradually increasing up to 1 Hz. The response from the accelerometers mounted in the fuselage is very fast and represents the elevator excitation correctly in phase and magnitude. From the strain gauge channels (RWING/LWING), which show bending moment of the wing at the liftwire, it is apparent that the magnitude of the high frequency inputs do not get transferred into the wing motion very well. This was another indicator that, for low-input frequencies, the rigid-body model may give acceptable results for control parameter estimation, whereas high-frequency inputs excite flexible modes of the tail boom (TAILUP signal). Similar flights were conducted in the yaw and roll axis of the aircraft. These data were not used for parameter estimation because of the low signal-to-noise ratio of the roll gyro output signal. By analyzing different sets of maneuvers out of the same test flight the parameter estimates did not converge for a number of reasons. The particular trajectories flown were not "exciting" enough. This means that the true effect of the maneuver was overpowered by unmodeled effects (such as nonlinearities of the aircraft, atmospheric turbulence, unsteady aerodynamics, and structural flexibility).

Rigid Aircraft Parameter Identification

Although the test flights and basic theoretical considerations suggest that flexibility effects of the structure and unsteady aerodynamics are both significant (especially when the control inputs are performed at high frequencies), the first attempt to estimate control and stability derivatives from small perturbation maneuvers was based on a rigid-body model with quasisteady aerodynamics.[6] Use of existing parameter estimation software at NASA Dryden Flight Research Facility [6,7] simplified this task. This software, pEst, uses equations of motion based on the assumption of rigid-body motion and quasisteady aerodynamics. The inputs (time histories of δ_E, δ_R) are given to the program as data as are the measured responses. The program iteratively adjusts a specified set of parameters in order to minimize the time-integrated squared difference between the measured and the simulated responses. Initial parameter estimates were generated by a computational method, which treats the aircraft as a rigid body and is able to model steady three-dimensional flow around the aircraft. Also known as QUADPAN, the method is described in more detail in Ref. 5. These parameters are used by pEst as starting values for the iteration. Several minimization algorithms are available: gradient, Newton-Raphson, and David-Fletcher-Powell.[6] Gradients and second gradients are calculated by finite differences.

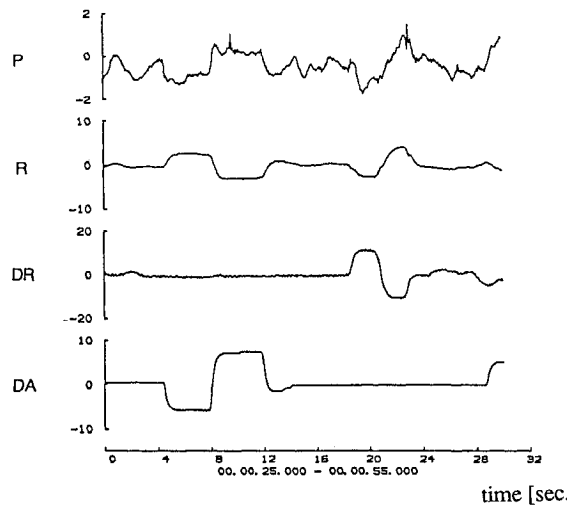

Fig. 6 Rudder and aileron doublet.

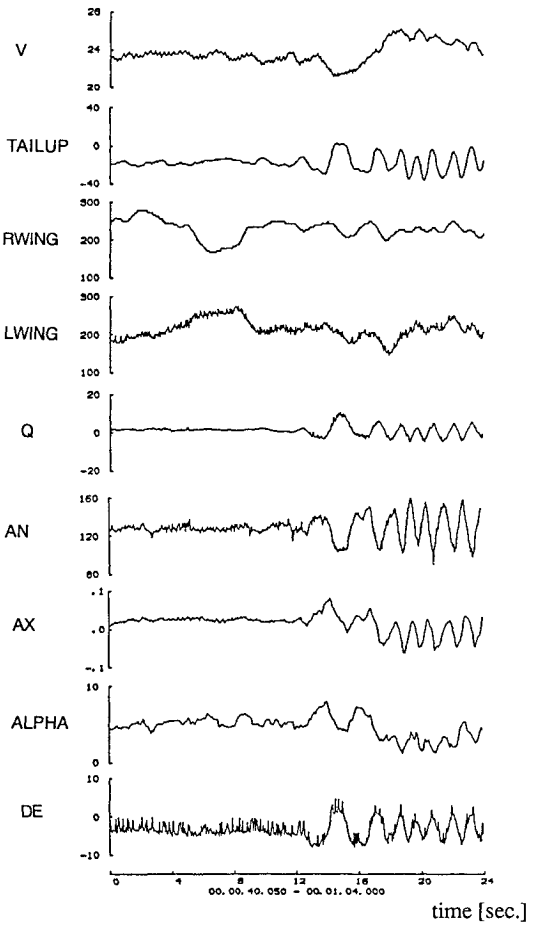

Fig. 7 Elevator frequency sweep.

Although the flight test maneuvers of the Light Eagle did not exceed the range of validity of linear theory, pEst, which implements kinematically nonlinear equations, was used for convenience. Specifically, for lateral maneuvers, the aircraft was modeled by

$$\dot{\beta} = p\sin\alpha - r\cos\alpha + \frac{\bar{q}S_R R}{mV}C_y + \frac{gR}{V} \times \left[\cos\beta\cos\theta\sin\phi - \sin\beta(\cos\theta\cos\phi\sin\alpha - \sin\theta\cos\alpha)\right]$$

$$I_x\dot{p} = \bar{q}S_R bC_l R + \left[qr(I_y - I_z)\right]/R$$

$$I_z\dot{r} = \bar{q}S_R bC_n R + \left[pq(I_x - I_y)\right]/R$$

$$C_y = C_{y_0} + C_{y\beta}\beta + \frac{b}{2VR}(C_{yr}r + C_{yp}p) + C_{y_{\delta R}}\delta_R$$

$$C_l = C_{l_0} + C_{l\beta}\beta + \frac{b}{2VR}(C_{lr}r + C_{lp}p) + C_{l_{\delta R}}\delta_R$$

$$C_n = C_{n_0} + C_{n\beta}\beta + \frac{b}{2VR}(C_{nr}r + C_{np}p) + C_{n_{\delta R}}\delta_R$$

where b is the reference span; c the reference chord; C_l the coefficient of rolling moment; $C_{l\beta}$, $C_{l_{\delta R}}$, C_{lr}, C_{l_0} rolling moment parameters; C_n the coefficient of yawing moment; $C_{n\beta}$, $C_{n_{\delta R}}$, C_{nr}, C_{n_0} the yawing moment parameters; C_y the coefficient of lateral force; $C_{y\beta}$, $C_{y_{\delta R}}$, C_{yr}, C_{y_0} the lateral force parameters; g the gravitational acceleration; I_x, I_y the moments of inertia; l the lever arm; m the mass; p the roll rate; q the pitch rate; α the angle of attack; β the angle of sideslip; θ the pitch attitude; ϕ the roll attitude; and δ_R the rudder deflection.

The cost function to be minimized, chosen based on available measurements, was

$$J(\zeta) = \frac{1}{2n_z n_t}\sum_{i=1}^{n_t}\left[z(t_i) - \tilde{z}(t_i,\zeta)\right]^T W\left[z(t_i) - \tilde{z}(t_i,\zeta)\right]$$

with

$$z = \left[\beta, p, r, a_y, \text{tail side}\right]^T$$

$$\zeta = \left[C_{y_0}, C_{y\beta}, C_{y_{\delta R}}, C_{yr}, C_{l_0}, C_{l\beta}, C_{l_{\delta R}}, C_{lr}, C_{n_0}, C_{n\beta}, C_{n_{\delta R}}, C_{nr}, \text{tail side}_{\text{bias}}\right]^T$$

where n_z, n_t are the number of time history points and response variables, z the measured response, $\tilde{z}$ the response computed by integrating the equations of motion, ζ the parameter vector, and superscript T the transpose.

The tail-side force response was modeled by ignoring contributions from the empennage mass, yaw rate, roll rate, and lateral acceleration.

$$\text{tail side} = \bar{q}S_R L\left(C_{y_{\delta R}}\delta_R + C_{y\beta}\beta\right) + \text{tail side}_{\text{bias}}$$

where l is distance from strain gauge to rudder hinge, δ_R the rudder deflection, and $\text{tail side}_{\text{bias}}$ the tail side force bias term.

Whereas the constants that define the mass of the aircraft, inertias, wing area, span, chord, and location of the aircraft center of gravity are well known, there are a large number of longitudinal and lateral-directional control and stability derivatives that are very poorly known and nearly impossible to predict analytically. Among them are some of the lateral-directional derivatives such as $C_{l\beta}$, C_{lp}, C_{lr}, $C_{n\beta}$, C_{np}, and C_{nr}.

Generally, the effect of some of these parameters (C_{lr}, C_{nr}, C_{lp}, C_{np}) is not significant for the overall behavior of typical aircraft, but in the case of extreme light wing loading, low Reynolds number airfoils, high aspect ratio, low flight speeds, and flexible structures, this may not be true. During the Light Eagle flight test program it was found, for instance, that the aircraft turns with much higher angles of sideslip than predicted and therefore parameters like $C_{l\beta}$ and $C_{n\beta}$ become very important. During the turn, much of the rolling moment is generated by C_{lr}—unusually important due to low flight speed and high aspect ratio.

In terms of estimating control and stability parameters from small perturbation maneuvers, it would be very optimistic to try to estimate too many parameters at a time. Therefore, a very common procedure is to reduce the number of free parameters considerably to about five or six. This process was followed, leading to an iterative procedure during which one flight test maneuver would be analyzed with different sets of free parameters. This leads to an understanding of the importance and the effects of these parameters on the performance of the mathematical model of the aircraft, and enhances convergence to a final model.

After having analyzed a number of parameters with either the same maneuver or the same group of maneuvers (rudder doublets), it became obvious that a time delay between rudder surface actuation and tail-side bending moment leads to contradictory results, and the validity of the rigid-body model came into question. Figure 8 shows time-history plots for a rudder doublet with most weight in the cost function J on yaw rate response, lateral acceleration, and sideslip angle. Roll-rate and tail-side bending moment were lightly weighted in order to improve the curve fit on the first three variables. Although the presented maneuver is one of the best that was performed throughout the entire flight test program, it is obvious that the tail-side bending moment is generated more slowly than is predicted by the model.

Model of Flexibility and Aerodynamic Lag

Inspection of Fig. 8 suggests that the computed tail-side bending moment response differs from the measured response by a simple lag. One might hypothesize this lag to be due to the response of an overdamped flexible degree of freedom between the control surface (the rudder) and the fuselage. Indeed, such flexibility is provided by the tail boom. Simple estimates of the damping ratio (using quasisteady aerodynamics) suggest that tail-boom lateral-bending motion experiences an aerodynamic damping of 20% of critical. The response of

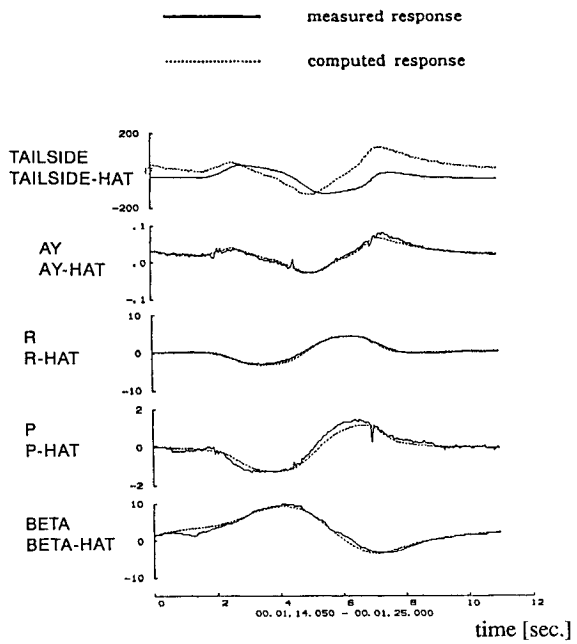

Fig. 8 The pEst results for rigid-body dynamics.

such a highly damped mode, with resonant frequency of 1.4 Hz, looks not unlike that of a first order lag with a time constant of 0.3 s. An alternative origin for this lag is aerodynamic; inspection of Fig. 6 shows that the rudder angle is increased nearly impulsively. Fung[8] gives a clear discussion of the the lift produced by an airfoil with a sudden change in angle of attack and shows that the unsteady lift is given by a time convolution of Wagner's function with downwash at the three-quarter-chord point. Wagner's function is well approximated by

$$\phi(T) = 1 - 0.165e^{-0.0455T} - e^{-0.3T}$$

$$T = \frac{2U_\infty t}{c}$$

This indicates a first-order aerodynamic lag with a time constant (based on rudder chord of $c = 0.7$ m; $U_\infty = 8$ m/s)

$$\tau = \frac{3.3c}{2U_\infty} = 0.14 \text{ s}$$

The lateral-directional equations of motion were thus extended to include a first-order filter between rudder deflection and application of the resulting torque on the fuselage

$$\dot{x}_{\text{lag}} = -\frac{1}{\tau}x_{\text{lag}} + \frac{1}{\tau}\delta_R$$

$$C_y = C_{y_0} + C_{y\beta}\beta + \frac{b}{2VR}(C_{yr}r + C_{yp}p) + C_{y_{\delta R}}x_{\text{lag}}$$

$$C_l = C_{l_0} + C_{l\beta}\beta + \frac{b}{2VR}(C_{lr}r + C_{lp}p) + C_{l_{\delta R}}x_{\text{lag}}$$

$$C_n = C_{n_0} + C_{n\beta}\beta + \frac{b}{2VR}(C_{nr}r + C_{np}p) + C_{n_{\delta R}}x_{\text{lag}}$$

$$\text{tail side} = \bar{q}S_R l(C_{y_{\delta R}}x_{\text{lag}} + C_{y\beta}\beta) + \text{tail side}_{\text{bias}}$$

Figure 9 shows the improvement of the curve fit on the tail-side bending moment after extending the lateral equations of motion in the above suggested manner with the same weights in W and τ_{start} iteration = 0.3 s. Table 6 presents a comparison between computed (QUADPAN) and estimated (pEst) control and stability parameters. The differences between the results suggest that the influence of the aircraft flexibility and unsteady aerodynamics is greater than originally expected.

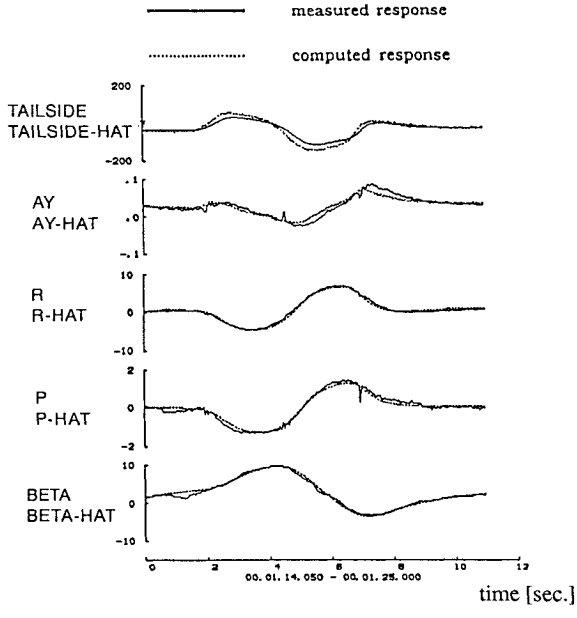

Fig. 9 The pEst results for extended equations of motion.

Parameter estimation is not yet finished. Only one set of maneuvers (rudder doublets) has been used to date. These results (and the qualitative discussion of the rudder frequency sweep given earlier) suggest that the rudder is incapable of applying torques to the aircraft with significant spectral content above a few Hz. A combination of aerodynamic lag and tail-boom flexibility prevent this. Similar limitations are anticipated with the ailerons and the elevator although data analysis is not yet complete.

Because of this spectral limitation of the aerodynamic actuation, and the apparent high damping in all the responses, a rigid-body model of the aircraft may have some applicability—particularly when augmented by low-pass filters. We visualize development of a flight-verified rigid-body model with selected validity. The model would be valid to high frequencies well into the range where unsteady aerodynamics and flexibility become important, however this validity would be restricted to excitations from the aerodynamic control surfaces and to currently measured responses. Such a model has utility for pilot handling evaluation or for autopilot design. It is, however, somewhat phenomenological and cannot predict other important aspects of aircraft response; flutter, gust response, and response of aircraft states not contributing to the cost function being minimized.

Fully Flexible Model of the Light Eagle

In order to provide an even better understanding of this unique aircraft, a fully flexible aeroelastic model is currently under development.[9] The model is being guided by the frequency estimates of Table 4. The analysis is marked by the approximate equality of many structural natural frequencies and by the anticipated importance of unsteady aerodynamic effects. The approach being taken uses assumed modes. The assumed modes are generated by eigenanalysis of the free-free aicraft with apparent mass loading but with no flight speed. It is difficult to justify inclusion or exclusion of any particular mode; no clear spectral separation between low-frequency and high-frequency modes has been identified.

Longitudinal and lateral analyses are performed separately, and convergence of the computed results with an increasing number of assumed modes is studied. This process is limited by computational capacity. Aerodynamics are modeled by modified strip theory and by evaluation of a transcendental Theodorsen's function.

Such an aeroelastic model, consistently including rigid-body, elastic, and aerodynamic states, is of high order and represents a significant computational extrapolation from experimentally verified results. Experimental validation will not be a trivial task. One might attempt a ground vibration test to

Table 6 Parameter estimation results

	Stability derivatives		
	QUADPAN	pEst	pEst (with lag terms)
C_{y0}	0.0000	0.4247E-01	0.3315E-01
$C_{y\beta}$	−0.7000E-02	−0.6262E-02	−0.4048E-02
$C_{y\delta r}$	0.5300E-02	0.4638E-02	0.3210E-02
C_{l0}	0.0000	−0.1353E-02	−0.1294E-02
C_{lb}	−0.1700E-02	−0.6493E-03	−0.1501E-02
C_{lp}	−0.7900	−0.2445	−0.7900
C_{lr}	−0.2110	−0.5667E-01	−0.1456
C_{n0}	0.0000	0.6056E-04	0.1651E-04
$C_{n\beta}$	0.6500E-03	0.1744E-04	0.1996E-03
$C_{n\delta r}$	−0.9500E-03	−0.8738E-02	−0.1197E-02
$a_{y\text{bias}}$	0.0000	−0.4829E-02	−0.3343E-02
τ	0.0000	0.0000	0.1700E-01

validate the model at zero flight speed, although the large apparent mass and damping make such a test difficult. The flight data collected so far may prove adequate for model validation, although special software will need to be written to handle the larger set of equations of motion. Additional flight tests with excitation schemes other than aerodynamic control surfaces may prove necessary to provide enough high frequency content and to identify parameters associated with the faster degrees of freedom. Novel excitation schemes might include weight drops, rockets, and bicyclists pulling on ropes. It seems likely that such a large model would never be validated entirely, but would have to rely partially on a theoretical basis.

IV. Summary and Conclusions

Although research continues into the modeling of the aircraft flexibility and into its participation in the dynamic response, we can draw several conclusions at this point. The large number of test flights over a period of three months enabled us to cover almost the whole flight envelope, although the high-speed region was not very well examined. The data acquisition system, instrumentation, telemetry, and recording system, developed by Daedalus team members, provided good quality data, which are probably unique with this type of aircraft and in this Reynolds number regime.

The augmentation of the aircraft lateral equations of motion (see Fig. 9) has yielded a model that is generally correct although limited in its applicability to the excitations and responses used during flight test. This especially addresses the question of convergence of the parameter estimates from different maneuver sets and the degree of excitation of unmodeled modes. The current model used for parameter estimation clearly shows these limits. Unfortunately the incompleteness of the model may lead to parameter estimates which are valid only for the specific maneuvers used for estimation.

A comparison between different turn maneuvers (with ailerons/with rudder only) showed that ailerons are ineffective. The large adverse yaw torque generated by aileron deflection causes yaw rates, which, through C_{lr}, tend to roll the aircraft against the direct aileron roll torque. The net effect is large adverse yaw rates and very small roll rates in the commanded direction.

This work has led to some insights for the flight test of highly flexible aircraft. Aerodynamic control surfaces may be inadequate for excitation into the frequency range of flexible response because of aerodynamic lag. A more complete model of aircraft flexibility is needed for an aeroelastic stability analysis, for gust response, and for predicting flutter boundaries. If such a model is to be verified in flight test, a means must be developed for high frequency excitation of the aircraft's structure. Parameter estimation with such an expanded model with flexible and aerodynamic states may introduce a new set of difficulties; it is not yet clear to what degree such a model can be verified in flight test.

References

[1]Hall, D.W., Fortenbach C. D., Dimiceli E. V., and Parks, R.W., "A Preliminary Study of Solar Powered Aircraft and Associated Power Trains," NASA CR-3699, Dec. 1983.

[2]Petre, A., and Ashley, H., "Drag Effects on Wing Flutter," *Journal of Aircraft,* Vol. 13, No. 10, 1976, pp. 755–763.

[3]Boyd, W. N., "Effect of Chordwise Forces and Deformations and Deformations due to Steady Lift on Wing Flutter," Ph.D. Thesis, Stanford University, Stanford, CA, SUDAAR No. 508, Dec. 1977.

[4]Chen, G. S., "Aeroelastic Behavior of Forward Swept Graphite/Epoxy Wing Aircraft with Rigid-Body Freedoms," Ph.D. Thesis, Massachusetts Institute of Technology, Cambridge, MA, Rept. 86-14, May 1986.

[5]Sullivan, R. B., and Zerweckh, S. H., "Results of the Flight Test Program with the Light Eagle and the Daedalus Aircraft," NASA Contractor Rpt., NASA Langley, Aug. 1988.

[6]Murray, J. E., and Maine, R. E., "pEst Version 2.1 User's Manual," NASA TM 88280, Sept. 1987.

[7]Maine, R. E., and Iliff, K. W., "MMLE 3 User's Manual," NASA TP 1563, Nov. 1980.

[8]Fung, Y. C., *An Introduction to the Theory of Aerolasticity,* Dover, New York, 1969.

[9]van Schoor, M., Zerweckh, S. H., and von Flotow, A. H., "Aeroelastic Stability and Control of a Highly Flexible Aircraft," *Journal of Aircraft* (to be published).